Low-Frequency Alfvén Eigenmodes during the Sawtooth Cycle at ASDEX Upgrade

D. Curran[1], Ph. Lauber[2], P.J. Mc Carthy[1], S. da Graça[3], V. Igochine[2]
and the ASDEX Upgrade Team[2]

[1] *Department of Physics, University College Cork, EURATOM-Association DCU, Cork,Ireland*

[2] *Max-Planck-Institut für Plasmaphysik, EURATOM-Association, Garching, Germany*

[3] *Associação EURATOM/IST, Instituto de Plasmas e Fusão Nuclear - Laboratório Associado, Insituto Superior Técnico, 1049-001 Lisboa, Portugal*

Introduction and Experimental Observations

Recent experiments at ASDEX Upgrade have demonstrated the appearance of low frequency modes in the range between that of the kink instability and toroidicity-induced Alfvén eigenmode (TAE). These modes appear to exist close to the $q = 1$ surface and have been observed during ICRH and NBI heated discharges. It is proposed that these modes are beta-induced Alfvén eigenmodes (BAEs). BAEs are electromagnetic, $n \neq 0$ perturbations that appear to be driven by strong gradients in temperature and density as well as by energetic particle popluations [1].

They occur in the low-frequency gap in the shear Alfvén continuum opened up by geodesic curvature and finite ion compressibility, which increases with beta. In addition to BAEs, modes which chirp upwards significantly in frequency towards the end of the sawtooth cycle have also been observed. This evolution of the extrema of the Alfvén continuum which has been proposed in [1] is investigated further in this work. Discharges 23824 and 25546 are considered, both of which exhibit mode activity characteristic of BAEs and are medium/high density discharges with $I_p \approx 800kA$. During the time-periods considered, 25546 is heated using 4.395MW ICRH while 23824 is heated using 4.66MW ICRH and 2.615MW NBI. During periods of ICRH and sawtooth activity, low-frequency mode activity is evident from SXR [2] and magnetics mea-

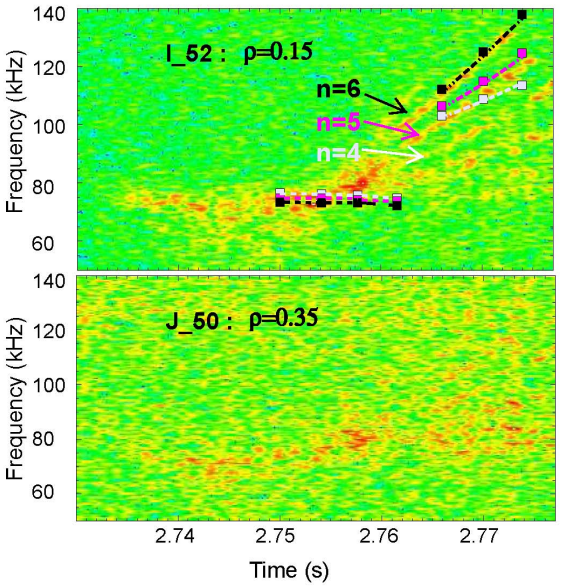

Figure 1. Chirping mode activity measured with soft X-ray diagnostic (SXR) during a sawtooth cycle of discharge 23824. Numerically calculated BAE ($t \approx 2.75 - 2.762$s) and chirping mode ($t \approx 2.766 - 2.774$s) frequencies for $n = 4 - 6$ overplotted.

surements close to and within the $q = 1$ surface. Figures 1 and 2 show mode activity during 23824 ad 25546, measured using SXR chords with tangency radii between $\rho_{pol} = 0.15 - 0.35$. For discharge 23824, SXR channels with tangency radii of $\rho_{pol} = 0.35$ and larger continue to show BAE mode activity while the chirping modes hardly evident. From this it can be inferred that the modes observed consist of two different types - the BAEs which are localized around the $q = 1$ surface, and core-localized chirping modes, similar to those observed in [1][3].

$q = 1$ surface locations were determined from the estimated sawtooth inversion radius to be $\rho_{pol} = 0.33$ and 0.45 for 25546 and 23824. In both discharges, the mode frequencies appear to dip during the early sawtooth cycle before recovering towards the end of the cycle. Mode number splittings are evident in 25546 and are estimated from magnetics to correspond to $n = 3,4,5$ and 6 in decreasing frequency order. These splittings and frequency dipping are not as evident in 23824 but the modes are believed to be caused by the same mechanism. The highest three mode numbers during the chirping mode phase ($t \approx 2.76 - 2.778$s) are estimated to correspond to $n = 4,5,6$ from magnetics.

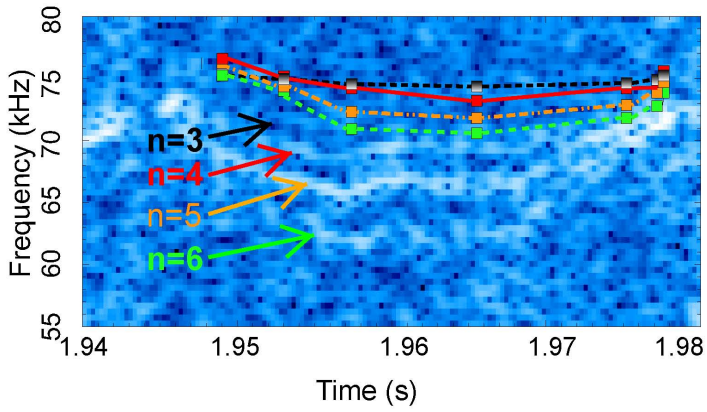

Figure 2. BAE mode activity measured with soft X-ray diagnostic (SXR) [2] during sawtooth cycle of discharge 25546. Numerically calculated mode frequencies for $n = 3 - 6$ overplotted.

Analysis and Results

In order to investigate this behaviour, a kinetic balooning mode dispersion relation was re-derived for the gyrokinetic model underlying the eigenvalue code LIGKA [1][4]. Keeping the $m \pm 1$ sidebands, retaining the geodesic curvature and the sound wave coupling by an appropriate approximation of the propagator integrals, leads to:

$$\omega^2(1-\frac{\omega_{*p}}{\omega}) - k_{\|m}^2 R_0^2 \omega_{A0}^2 = 2\sqrt{\frac{2}{1+\kappa^2}}\frac{\upsilon_{thi}^2}{R_0^2\omega_{A0}^2}(-[H(x_{m-1})+H(x_{m+1})]+ \tau[\frac{N^m(x_{m-1})N^{m-1}(x_{m-1})}{D(x_{m-1})}+\frac{N^m(x_{m+1})N^{m+1}(x_{m+1})}{D(x_{m+1})}])$$

where $x_m = \frac{\omega}{k_{\|m}\upsilon_{th}}$, $\upsilon_{thi}^2 = \frac{2T_i}{m_i}$, $\omega_{*p} = \omega_{*n} + \omega_{*T} = \frac{T_i}{eB}k_\theta(\frac{\nabla n}{n})(1+\eta)$ with $\eta = \frac{\nabla T}{T}/\frac{\nabla n}{n}$ and D, H and N representing the sound wave, geodesic curvature and coupling terms respectively. The equation has been modified in order to take account of plasma elongation effects [5]. Equilibrium reconstructions were generated using the CLISTE code [6] for time-points during 23824 and 25546 in order to obtain fitted q-profiles. An estimate for the minimum on-axis safety factor

value q_0 was obtained from mode frequency and mode number data. This was assumed to fall from $q_0 = 1.00$ to the $q_0 \approx 0.96$ estimate during the sawtooth cycle. This estimate, as well as the $q = 1$ surface information was used to constrain the q-profiles. The plasma elongation was determined to be approximately $\kappa = 1.3$ in the region of interest. Ion density profile information was obtained through the availability of a Z_{eff} profile [7]. A reliable determination of the plasma rotation frequency was not possible so conservative estimates of $f_{rot} = 1.5$kHz were taken. Mode number and temperature gradient variations appear to have a strong effect on BAE frequency close to $q = 1$ surface. Thus, the diamagnetic frequency ω_{*p} appears to be a major factor determining the BAE evolution during the sawtooth cycle as $\omega_{*p} \propto n\nabla T_e$. Figure 3 shows the electron temperature gradient ∇T_e evolution at the $q = 1$ surface, obtained from an integrated data analysis of the ECE and Thomson scattering diagnostics [8], during the course of the sawtooth cycle for 25546. This increases as the cycle progresses before decreasing towards the end. The degree to which the mode activity depends on ω_{*p} can be seen by comparing the evolution of ∇T_e and the mode frequencies for the two discharges in figures 3 and 4. The difference in maximum and minimum T_e gradients at the $q = 1$ surface is nearly three times greater for 25546 than it is for 23824 with the corresponding change in BAE mode frequency being significantly greater in 25546. It should be noted that the modes sit slightly below the accumulation point, so they will be subject to a further slight downshift in frequency. The calculated mode frequency is also several kHz higher than that obtained with a full numerical calculation due to the truncation of higher order terms in the derivation of the analytical expression.

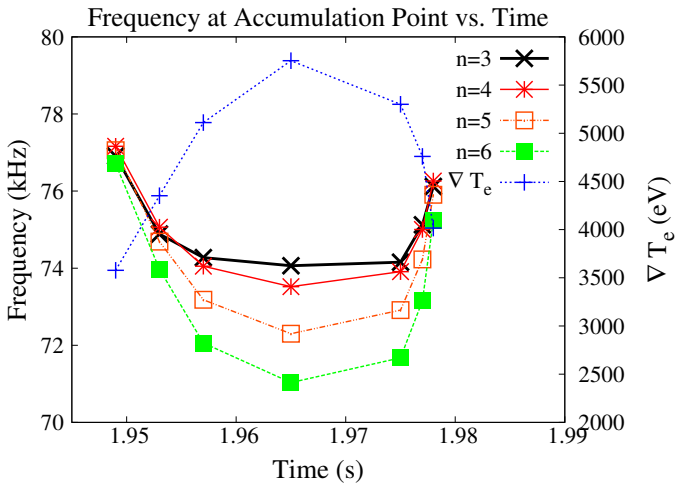

Figure 3. Comparison of calculated mode frequency at accumulation point with changes in electron temperature gradient at $q = 1$ surface during sawtooth cycle for discharge 25546.

A 25% downshift has been assumed in the mode frequency due to the effects of trapped particle dynamics on low frequency modes. This has been verified by full numerical calculations of the frequency continuum [9] [10]. It was intended to include terms governing the trapped particle effects in the calculations used in this work. This was unfortunately not possible by the time of submission but is planned for inclusion in future work. In discharge 23824, no clear mode splitting is evident in Figure 1 until $t \approx 2.76$s when chirping mode behaviour becomes active, reaching frequencies up to nearly 140kHz. Comparing the frequency of the BAE

accumulation point close to the $q = 1$ surface with the SXR measurements it was found that it can only explain the occurence of the earlier mode activity as the temperature gradients are not sufficient to explain such a drastic up-chirp in frequency later in the cycle.

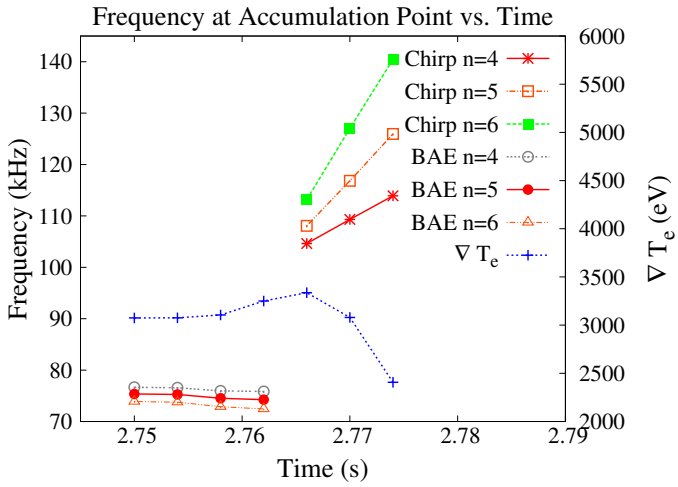

Figure 4. Comparison of calculated mode frequency at BAE and chirping mode accumulation points with electron temperature gradient at $q = 1$ surface during sawtooth cycle for discharge 23824.

Subsequent chirping mode activity can only be explained by assuming that a new continuum accumulation point is being observed which is more core localized, suggesting that it could be caused by changes in q_0. A comparison between the experimental and numerical values for the BAE and chirping mode frequencies are shown in figure 1, with q_0 assumed to vary linearly from $q_0 = 0.978 - 0.961$ for $t = 2.766 - 2.774$s. For $n = 4 - 6$ the numerically calculated slopes and magnitudes of the chirping mode frequencies appear to agree reasonably well with experiment.

Conclusion

It has been demonstrated that BAE mode activity is heavily dependant on temperature gradients in the plasma, and hence on the diamagnetic frequency. Better agreement is hoped to be found with experiment once an explicit expression for trapped particle effects, which are also dependant on ω_{*p}, is included. As the assumption of $T_i = T_e$ has been made, the availability of T_i profile data may also improve agreement with experiment in future calculations. Further, it has been shown that the on-axis safety factor value q_0 plays an important role in determining the evolution of low frequency core-localized chirping modes.

References

[1] Ph. Lauber et al, Plasma Phys. Control. Fusion, **51** (2009)
[2] V. Igochine et al, IPP Report 1/338 (2010)
[3] A.G. Elfimov et al, Plasma Phys. Control. Fusion, **53** (2011)
[4] F. Zonca et al, Plasma Phys. Control. Fusion, **38**, 2011 (1996)
[5] Z. Gao et al, Nucl. Fusion, **49**, 045014 (2009)
[6] P.J. Mc Carthy, Phys. Plasmas, **6**, 3554 (1999)
[7] S.K. Rathgeber et al, Plasma Phys. Control Fusion, **52** (2010)
[8] R. Fischer et al, Fusion Science Technology, **58** 2 (2010) 675-684
[9] Ph. Lauber et al, Proc. of the 23rd IAEA Fusion Energy Conference, Daejon, Korea Rep. of (IAEA, Vienna), Vol. IAEA-CN-180 (2010), THW/2-2Ra
[10] I. Chavdarovski and F. Zonca, Plasma Phys. Control. Fusion **51** (2009) 115001